

## Adsorption of Ciprofloxacin using Composite Film from PVA, Agarose and Maltodextrin

(Penjerapan Ciprofloksacin menggunakan Filem Komposit daripada PVA, Agarosa dan Maltodekstrin)

BICH NGOC HOANG<sup>1,2</sup>, HUONG DIEU TRAN<sup>3,4</sup>, THI CAM QUYEN NGO<sup>1,2</sup>, NGUYEN THI NHU DUNG<sup>5</sup> & LONG GIANG BACH<sup>1,2,\*</sup>

<sup>1</sup>*Institute of Applied Technology and Sustainable Development, Nguyen Tat Thanh University, Ho Chi Minh City, Vietnam*

<sup>2</sup>*Faculty of Food and Environmental Engineering, Nguyen Tat Thanh University, Ho Chi Minh City 700000, Vietnam*

<sup>3</sup>*Faculty of Chemical Engineering, Ho Chi Minh City University of Technology (HCMUT), 268 Ly Thuong Kiet, District 10, Ho Chi Minh City, Vietnam*

<sup>4</sup>*Vietnam National University Ho Chi Minh City, Linh Trung Ward, Thu Duc District, Ho Chi Minh City, Vietnam*

<sup>5</sup>*Ho Chi Minh City University of Natural Resources and Environment (HCMUNRE), Vietnam*

*Received: 16 December 2022/Accepted: 19 June 2023*

### ABSTRACT

Antibiotic resistance is one of the most alarming problems today. Therefore, composite membranes have been widely applied for the removal of antibiotics from water. PVA/Agarose/Maltodextrin films have been synthesized by casting with various component ratios. They were evaluated for characteristics through moisture, solubility, expansion, and BET results. The results showed that PVA/Agarose/Maltodextrin films exhibited the best viability in the aquatic environment through low solubility ( $68.88\% \pm 0.03$ ), high swelling ( $431.77\% \pm 5.89$ ) and pore volume ( $0.034969 \text{ cm}^3/\text{g}$ ). The adsorption capacity of PVA/Agarose/Maltodextrin was tested for several antibiotics such as Ciprofloxacin, Tetracycline, Oxy-Tetracycline, and Chloramphenicol. The results showed that Ciprofloxacin was removed by the PVA/Agarose/Maltodextrin films better than other antibiotics. The highest antibiotic adsorption was obtained at 20 min, temperature of  $30 \text{ }^\circ\text{C}$ , dosage of  $2 \text{ g/L}$ , pH 6, and antibiotic concentration of  $40 \text{ mg/L}$ . Ciprofloxacin adsorption was predicted through adsorption kinetic and isothermal models. The compatibility of the Pseudo First Order kinetic and Dubinin-Radushkevich isothermal has shown that adsorption takes place according to a physical adsorption mechanism with electrostatic interactions on the surface of the material. The maximum adsorption capacity recorded at  $4.48 \text{ mg/g}$  based on the Dubinin-Radushkevich isothermal.

Keywords: Agarose; Ciprofloxacin; composite membrane; Maltodextrin; PVA

### ABSTRAK

Rintangan antibiotik ialah salah satu masalah yang paling membimbangkan hari ini. Oleh itu, membran komposit telah digunakan secara meluas untuk penyingkiran antibiotik daripada air. Filem PVA/Agarosa/Maltodekstrin telah disintesis dengan tuangan dengan pelbagai nisbah komponen. Ia dinilai untuk ciri melalui kelembapan, keterlarutan, pengembangan dan keputusan BET. Keputusan menunjukkan bahawa filem PVA/Agarosa/Maltodekstrin mempamerkan daya maju terbaik dalam persekitaran akuatik melalui keterlarutan rendah ( $68.88\% \pm 0.03$ ), bengkak tinggi ( $431.77\% \pm 5.89$ ) dan isi padu liang ( $0.034969 \text{ cm}^3/\text{g}$ ). Kapasiti penjerapan PVA/Agarosa/Maltodekstrin telah diuji untuk beberapa antibiotik seperti Ciprofloksacin, Tetracycline, Oxy-Tetracycline dan Chloramphenicol. Keputusan menunjukkan bahawa Ciprofloksacin telah dikeluarkan oleh filem PVA/Agarosa/Maltodekstrin lebih baik daripada antibiotik lain. Penjerapan antibiotik tertinggi diperoleh pada 20 minit, suhu  $30 \text{ }^\circ\text{C}$ , dos  $2 \text{ g/L}$ , pH 6 dan kepekatan antibiotik  $40 \text{ mg/L}$ . Penjerapan Ciprofloksacin telah diramalkan melalui model kinetik dan isoterma penjerapan. Keserasian kinetik Pseudo First Order dan isoterma Dubinin-Radushkevich telah menunjukkan bahawa penjerapan berlaku mengikut mekanisme penjerapan fizikal dengan interaksi elektrostatik pada permukaan bahan. Kapasiti penjerapan maksimum direkodkan pada  $4.48 \text{ mg/g}$  berdasarkan isoterma Dubinin-Radushkevich.

Kata kunci: Agarose; Ciprofloksacin; membran komposit; Maltodekstrin; PVA

## INTRODUCTION

The rapid development of aquaculture has been posing immediate and long-term environmental problems such as biological imbalance, the risk of environmental pollution, and the development of diseases (Kumar et al. 2005; Mishra et al. 2019). The mis-use antibiotics in aquaculture regarding types, doses, and time affects the quality of aquatic products as well as has a negative impact on their disease resistance, and the environment (Mirasgedis et al. 2008; Ololade et al. 2019; Przydatek & Kanownik 2019). Previous studies have shown that wide range of antibiotics have been used for aquaculture, including Ciprofloxacin, Amoxicillin, Chloramphenicol, Tetracycline, Enrofloxacin, Oxytetracycline which had significant effects on public health and the environment (Ding & He 2010; Lulijwa, Rupia & Alfaro 2020). Antibiotic residues removal has been interesting to many domestic and foreign scientists. Currently, there are many methods to treat antibiotic residues such as adsorption (Abd El-Monaem et al. 2022b), photocatalyst (Janani et al. 2022), and Advanced Oxidation (Boczkaj & Fernandes 2017). Adsorption is one of the highly effective and sustainable methods for developing countries due to the use of affordable and natural-derived adsorbent materials (Abd El-Monaem et al. 2022b). Therefore, the fabrication and modification of adsorbent materials and applications for antibiotic removal in the aquatic environment are necessary and have great scientific significance in the current period.

Membranes used in adsorption processes have been developed rapidly in recent years due to their specific adsorption performance, potential for environmental friendliness, the generation of no secondary pollutants, as well as high energy efficiency and quantity (Zhao et al. 2020). Membranes with porous structures have been fabricated from organic and inorganic materials. Organic films are the most popular adsorbents due to their controllable chemical stability, hydrophobicity or hydrophilicity, excellent chemical reactivity with mechanical strength, and different volumes of electrical groups (Gao et al. 2019; Rodríguez-San-Miguel & Zamora 2019; Zhao et al. 2020). Due to the special adsorption properties of charge-carrying polymers on the surface of solid materials, many polymers have been used to modify the surface of materials to improve the efficiency of organic pollutant removal (Ramakrishna et al. 2001). Charge-carrying polymers are generally divided into negatively and positively charged polymers. Charged polymers have various applications in the coatings industry, resist corrosion, and act as coagulants

(Bailey & Winey 2020; Dhand et al. 2015; Fu et al. 2019). They are also widely used in environmental remediation and removal of Ciprofloxacin, Tetracycline, Amoxicillin, Oxytetracycline, and Doxycycline (Chang et al. 2021; Hami et al. 2019; Hamoudi, Hamdi & Brendlé 2021; Lu et al. 2017; Wu et al. 2019; Yazidi et al. 2020; Yan et al. 2020). Specifically, PVA is known as a negatively charged and environmentally friendly polymer with its outstanding properties, hence being widely applied in different industries and used as adsorbent materials for the treatment of pollutants.

Recently, PVA has been widely used for wastewater treatment applications because of its compatibility, non-toxicity and biodegradability (Abdeen, Mohammad & Mahmoud 2015; Mahdavinia et al. 2014). However, PVA's strong affinity for water molecules, which can degrade the performance of materials and lose their integrity, limits the use of PVA in water purification (Chen et al. 2018; Figueiredo, Alves & Borges 2009). To date, many methods have been proposed to reduce the hydrophilic properties of PVA films by cross-linking PVA by heat treatment, chemical agents (e.g., glutaraldehyde, glyoxal, boric acid, and clay) and physical processes (UV and electron beam irradiation) (Chen et al. 2018; Ghemati & Aliouche 2014). In 2022, chitosan-polycaprolactone membranes were used to treat tetracycline hydrochloride (Ghazalian et al. 2022). In addition, Abd El-Monaem et al. (2022a)'s research group used cellulose acetate and MOF materials to form films to treat tetracycline antibiotics. For example, for the treatment of tetracycline, the combinations of PVA with sodium alginate, chitosan + CuO + ZnS, and agarose to form foundation membrane and composite films have shown significant effectiveness (Chang et al. 2021; Dieu & Hoang 2021; Janani et al. 2022; Liao et al. 2022). It can be seen that tetracycline treatment with composite membranes from PVA is quite limited. Due to the water solubility of PVA, agarose and maltodextrin are added as crosslinkers and stabilizers for composite films (Hoang et al. 2020). In this study, the PVA membrane was combined with Agarose and Maltodextrin to evaluate the antibiotic removal potential.

## MATERIALS AND METHODS

### CHEMICALS AND REAGENTS

Poly vinyl alcohol (PVA) ( $M = 160,000$  g/mol) with a solubility of 86.5 - 89%, and Maltodextrine (GRM1249) are products of HIMEDIA company (Mumbai, India). Chloramphenicol (CPR), Ciprofloxacin (CFX),

Tetracycline (TCC), and Oxytetracycline (OTC) were obtained from Sigma-Aldrich, (St Louis, MO, USA). Agarose powder was manufactured by VWR BHD Prolabo Chemicals (Singapore).

#### PREPARATION OF COMPOSITE MEMBRANE

The film was synthesized by casting method based on our's previous studies (Hoang et al. 2020). Based on previous studies, samples were synthesized at different component ratios (w/w) ( Table 1) (Bich et al. 2021a; Hoang et al. 2020; Nguyen et al. 2021). Components were dissolved in 100 mL of distilled water at 50 °C. After mixing the 3 solutions, 0.5% glycerol (v/v) was added to the mixture and homogenized for 1 h using a magnetic stirrer. The film was then formed by pouring on a mold and dried at 45 °C for 48 h. The materials were dried at 40 °C before characterization (Hoang et al. 2020).

#### SOLUBILITY AND SWELLING

The solubility and swelling of the films were determined according to the method of Jipa, Stoica-Guzun and Stroescu (2012) and Wang et al. (2018). The film was cut to a size of 2 cm × 2 cm and recorded as the weight ( $M_1$ ) on the analytical balance of four odd numbers (PA214 Ohaus) before into the drying cabinet at 70 °C for 24 h. After drying, the film was re-weighed with dry mass ( $M_2$ ). The membrane samples were then placed in a petri dish containing 30 mL of milli-Q water for 24 h at room temperature and re-weighed in volume ( $M_3$ ). Samples were dried at 70 °C for 24 h and weighed

in mass ( $M_4$ ). Solubility and swelling were calculated as follows:

$$\text{Solubility (\%)} = \frac{M_2 - M_4}{M_2} \times 100 \quad (1)$$

$$\text{Swelling (\%)} = \frac{M_3 - M_2}{M_2} \times 100 \quad (2)$$

where  $M_1$  is the film weight before drying (g);  $M_2$  is the film weight after drying (g);  $M_3$  is the mass after immersion (g);  $M_4$  is the mass after second drying (g).

#### CHARACTERIZATION

The morphology of the film was measured by ultra high resolution scanning electron microscopy (FE-SEM) from Hitachi S-4800, Japan. The Nicolet 6700 spectrometer (FTIR) was used run and identified surface functional groups in the material's structure in the range of 4000  $\text{cm}^{-1}$  – 400  $\text{cm}^{-1}$ . X-ray diffraction patterns (XRD) were measured using a Sie-mens D5000 Diffrometer at a scan rate of 2°/min (2 $\theta$ ) with CuK (1.5406Å) radiation. Brunauer–Emmett–Teller (BET) theory was used to measure the surface area, pore volume, and pore size by MicroActive for TriStar II Plus 2.03 (Micromeritics Corporate Headquarters, USA). The analysis was performed through  $\text{N}_2$  capture by adsorption/desorption with 1  $\text{g}/\text{cm}^3$  degassed material at 150 °C for 12 h and the isothermal equation. The composite films were evaluated for hydrophobicity and hydrophilicity using a contact angle measuring device (KSV Instruments, USA).

TABLE 1. Sample name by component ratio

Sample name	Component ratio (%)			Reference
	PVA	Agarose	Maltodextrin	
PVA	100%	0%	0%	(Hoang et al. 2020)
PVA/Agarose	50%	50%	0%	
PVA/Maltodextrin	50%	0%	50%	
PVA/Agarose/Maltodextrin	20%	40%	40%	

### ADSORPTION EXPERIMENT

A total of 0.1 g/L – 3 g/L of composite film material was added to 100 mL of antibiotic (concentration 0 mg/L – 60 mg/L) in Erlenmeyer flask. The antibiotic solutions were prepared by diluting antibiotics in distilled water at different concentrations. The mixture's material and dye solution were shaken on a Thermal Incubation Shaker at 200 rpm at 30 °C - 60 °C from 0 min - 180 min. The antibiotic solutions were analyzed by an UV-VIS spectrophotometer (Shimadzu-1601 PC spectrophotometer, Japan) to record the concentration value with the corresponding wavelengths such as Tetracycline (273 nm), Ciprofloxacin (275 nm), Oxytetracycline (275 nm), and Chloramphenicol (280 nm). The dye adsorption capacity ( $Q_e$ ) was calculate according to the Equation (1):

$$Q_e = \frac{(C_o - C_e)}{W.V} \quad (3)$$

where  $C_e$  is the after-adsorption concentration (mg/L);  $C_o$  is the before-adsorption concentration (mg/L);  $W$  (g) is the adsorbent's mass; and  $V$  (L) is the solution's volume.

### THE ACIDS/BASES SURFACE AND ZETA POTENTIAL MEASUREMENT (pHpzc)

The point of zero charges (pzc), which is defined as at the pH level at which the net charge of the total surface of the particle is zero (Khandaker et al. 2018; Saha et al. 2020). Determination of pHpzc of materials followed the previously described procedure (Hoang et al. 2021, 2020). Briefly, KCl (0.1M) was adjusted the pH index at different pH ranging from 2 to 10 adjusted by HCl (1 mol/L) and NaOH (0.1 mol/L). A total of 50 mg of material was added to a flask containing 100 mL of the calibrated KCl solution. The pH values were noted to be initial and final. The final pH was measured and stirred for 48 h at room temperature.

### ADSORPTION KINETICS

Kinetic models are assume for the adsorption process and reaction rates for adsorption film. Experimental data were effectuated and described on kinetic models such as Elovich, Bangham, pseudo-first-order (PFO), and pseudo-second-order (PSO) in the following non-linear forms (Tran et al. 2017):

$$q_t = \frac{1}{\beta} \ln(1 + \beta t) \quad (4)$$

$$q_t = k_B t^B \quad (5)$$

$$q_t = q_e(1 - e^{-k_1 t}) \quad (6)$$

$$q_t = \frac{q_e^2 k_2 t}{1 + k_2 t q_e} \quad (7)$$

where  $q_t$  (mg/g) is the adsorption capacity at time  $t$ ;  $\beta$  is the desorption rate;  $\alpha$  is the chemical absorption rate;  $k_B$  and  $\alpha_B$  are Bangham constants;  $k_1$  (1/min) and  $k_2$  (g/(mg.min)) are the rates constant for pseudo-first-order, and pseudo-second-order;  $q_e$  (mg/g) is the adsorption capacity at the equilibrium..

### ADSORPTION EQUILIBRIUM ISOTHERM

Isotherm is the basis for considering the interaction between adsorbents and adsorbents in gas/liquid/solid interfaces. The adsorption processes are provided by the adsorption isotherms. The advantages and behavior of adsorption processes were precisely described by isothermal models such as Langmuir, Freundlich, Temkin, and Dubinin-Radushkevich (Ghaffari et al. 2017). Models are calculate in the following non-linear forms:

$$q_e = \frac{q_m K_L C_e}{1 + K_L C_e} \quad (R_L = \frac{1}{1 + K_L C_e}) \quad (8)$$

$$q_e = K_F C_e^{1/n} \quad (9)$$

$$q_e = B_T \ln \ln (k_T C_e) \quad (B_T = \frac{RT}{b}) \quad (10)$$

$$q_e = Q_m e^{-b t^2} \quad (\Sigma = RT \cdot \ln(1 + \frac{1}{C_e}); e = \frac{1}{\sqrt{2b t}}) \quad (11)$$

where  $C_e$  (mg/L) is the dye's equilibrium concentration; (mg/g) is the maximum adsorption capacity and (mg/g) is the adsorption capacity at the time of equilibrium;  $K_L$  (L/mg),  $K_T$  (L/g) and  $K_F$  [(mg/g).(L/mg)<sup>n</sup>] are constant Langmuir, Temkin and Freundlich;  $R_L$  is dissociation coefficient;  $1/n$  with  $n < 1$  (one-layer adsorption) and  $n > 1$  (multi-layer adsorption). In Temkin equation, the correlation coefficients  $B_T$  and isothermal constants  $b$  (L/mol). In Dubinin-Radushkevich equation,  $e$  (KJ/mol) is the adsorption energy,  $\epsilon$  is the Polanyi potentiality described and  $b_t$  ( $Mol^2/Kj^2$ ) is the Dubinin-Radushkevich constant.

## RESULTS AND DISCUSSION

## HYDROPHILIC AND HYDROPHOBIC PROPERTIES OF COMPOSITE MEMBRANE

Hydrophobicity/hydrophilicity was evaluated through parameters such as contact angle, solubility, moisture, and swelling. As shown in Figure 1(A), the solubility decreased from 100% to 68%. For PVA and PVA/Maltodextrin membrane, the swelling could not determine because the solubility reached 100%. The rapid dispersion of PVA and PVA/Maltodextrin in an aqueous medium demonstrates the high hydrophilic properties of PVA. The high hydrophilic properties of PVA have been demonstrated in many previous studies (Aslam, Kalyar & Raza 2018; Asrofi et al. 2019). The result shows that PVA/Agarose/Maltodextrin composite membranes has the lowest solubility ( $68.88\% \pm 0.03$ ), and high swelling ( $431.77\% \pm 5.89$ ), which indicates the formation of water-hydro polymer interactions (Madera-Santana, Freile-Pelegrín & Azamar-Barrios 2014; Yang et al. 2008). The high degree of swelling found in PVA/Agarose/Maltodextrin membranes implies that such membranes are less hydrophilic than PVA/Agarose. The component membrane results show that PVA and PVA/Maltodextrin membrane gave contact angles of  $42^\circ$  and  $44^\circ$ , respectively (Figure 1(B)). The  $50^\circ$  contact angle of PVA/Agarose membrane was improved compared to the original component film when combined with agarose. Membranes tend to have reduced hydrophilicity.

The PVA/Agarose/Maltodextrin membrane, the contact angle was markedly improved from  $50^\circ$  to  $90^\circ$ , along with reduced hydrophilicity. It can be seen as an excellent combination of three components PVA, Agarose and Maltodextrin. This demonstrates that the hydrophilicity of the membrane is strongly decreased when there is a combination of components. Low hydrophilicity makes the material stay in the water longer. Similar findings were reported by Sabarish and Unnikrishnan (2018) which used the combination of PVA membrane and zeolite. Overall, a small contact angle indicates high hydrophilicity and vice versa (Falath, Sabir & Jacob 2017).

## STRUCTURAL AND CHARACTERISTIC PROPERTIES OF PVA/AGAROSE/MALTODEXTRIN COMPOSITE MEMBRANE

The PVA/Agarose/Maltodextrin composite membrane was able to survive in water longer than the component membranes. Therefore, the PVA/Agarose/Maltodextrin composite membrane's structural characteristics were analyze by SEM, XRD, FTIR, and BET. The surface morphology and cross-section of the materials were analyze through SEM images (Figure 2). The SEM results of PVA show that the material has a flat surface and no blistering due to water vapor accumulation. The cross-section of the PVA shows a uniform mass without the formation of pores. The PVA/Maltodextrin film showed small bubbles on the surface and the

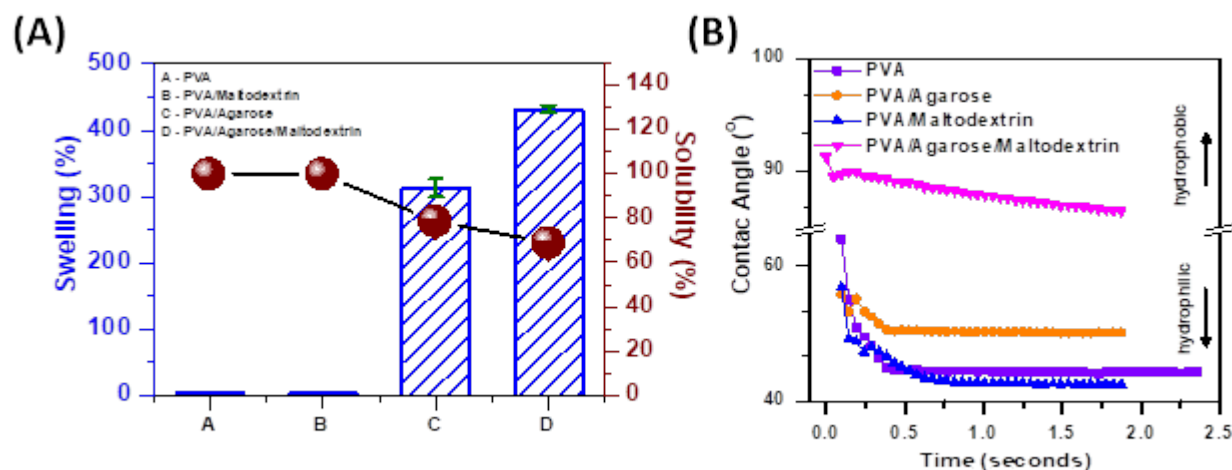


FIGURE 1. Solubility and swelling content (A), contact angle (B) of PVA, PVA/Maltodextrin, PVA/Agarose, and PVA/Agarose/Maltodextrin composite membrane

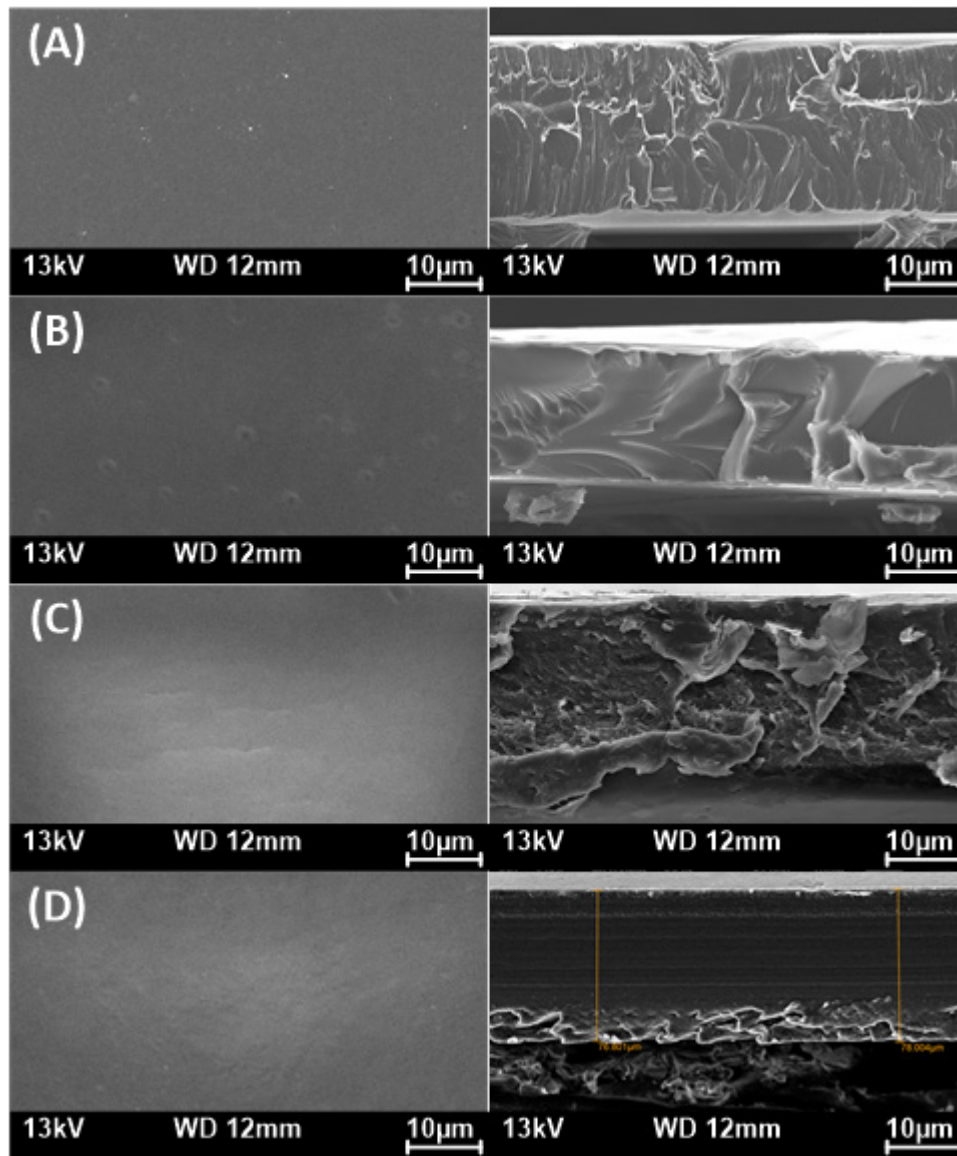


FIGURE 2. Scanning electron microscopy (SEM) images of the cross-section and surface of PVA (A), PVA/Maltodextrin (B), PVA/Agarose (C), PVA/Agarose/Maltodextrin (D) membrane

cross-section still showed a uniform mass without pore formation. In contrast, PVA/Agarose and PVA/Agarose/Maltodextrin membranes showed pore formation in the cross-sectional view and the flat membrane surface did not contain small bubbles. The appearance of pores when incorporating agarose component has also been demonstrated in Uppuluri and Shanmugarajan (2019)'s study. The cross-section with cracks and crevices

indicates the formation of voids of the PVA/Agarose/Maltodextrin film. The size of the membrane had been recorded with a thickness of about 76.3  $\mu\text{m}$ .

The functional groups of the surface and the structure of the membrane were analyzed by Fourier transform infrared (FTIR). The FTIR results are shown in Figure 3(A). The bands about  $3278\text{ cm}^{-1}$  and  $1600\text{ cm}^{-1}$  are attributed to the stretching and bending oscillations

of the OH group, respectively. The absorption peaks at  $2900\text{ cm}^{-1}$  and  $1253\text{ cm}^{-1}$  are assigned to the asymmetric stretching and bending of the C-H group, respectively. In addition, the intensity of the C-O stretching oscillation peak ( $1038\text{ cm}^{-1}$ ) was significantly increased compared with pure PVA. The characteristic oscillation peaks of pure PVA were found to be similar to those previously reported (Hoang et al. 2020; Rynkowska et al. 2019). The  $929\text{ cm}^{-1}$  peak exhibits the structural features of the C=C group motion of the PVA framework at the Trans binding site (Nawar & El-Mahalawy 2020). The stretching vibrations of the C-H group, C-O-C stretching vibrations were also observed at  $1342\text{ cm}^{-1}$ , and  $1149\text{ cm}^{-1}$ , respectively. It exhibits the structural properties of agarose (Shamsuri & Daik 2013). The peaks less than  $1000\text{ cm}^{-1}$  indicate the carbohydrate structure of maltodextrin (Maqsoudlou et al. 2020; Sritham & Gunasekaran 2017). Besides, Tian et al. (2017) reported the existence of hydrogen interactions between PVA and starch components, implying successful cross-linking of PVA. Therefore, partial blocking of the hydroxyl group in PVA by hydrogen bonding bridge in the composite film can reduce the affinity of PVA for water, which corresponds to a significant decrease in the solubility of the PVA film (Hoang et al. 2021, 2020; Nguyen et al. 2021; Yang et al. 2018). This behavior can improve its physical properties for application in aquatic environment. The X-ray diffraction (XRD) and SEM results were shown in Figure 3(B). The XRD results

of the PVA film showed a peak at  $2\theta = 19.4^\circ$  showing the amorphous structure of PVA. When combined with Maltodextrin, a small shoulder below  $15^\circ$  indicate the presence of maltodextrin inside the membrane. The XRD results of PVA/Agarose and PVA/Agarose/Maltodextrin membrane showed two distinct peaks at  $2\theta = 14.3^\circ$  and  $19.4^\circ$ , which were typical for PVA and agarose in the membrane's composition. With the amorphous structure, the arrangement of the polymer molecules was unclear. The results shown the amorphous structure of the material and had been demonstrated in previous studies (Hoang et al. 2021, 2020; Nguyen et al. 2021).

Due to the formation of pores from cross-sectional images, PVA/Agarose/Maltodextrin film was selected to evaluate specific surface area and pore volume.  $\text{N}_2$  and BJH adsorption-desorption methods are popular methods to investigate the pore structure and pore size distribution for membrane materials. From the BET results, the surface area of the membrane was recorded as  $5.9528\text{ m}^2\cdot\text{g}^{-1}$  with a pore size of about  $17\text{ nm}$ , the pore volume was recorded as  $0.034\text{ cm}^3\cdot\text{g}^{-1}$  (Figure 4). The adsorption isotherm of the PVA film was type II, with hysteresis to be type  $\text{H}_3$  in between adsorption and desorption branches. This shows that the first and second steps were monolayer adsorption and multilayer condensation, respectively. Hysteresis was wedge-shaped with open ends. Similar results had been demonstrate for composite films from PVA substrates (Ge et al. 2021). The BET measurement helps to predict the process and the adsorption capacity of the material.

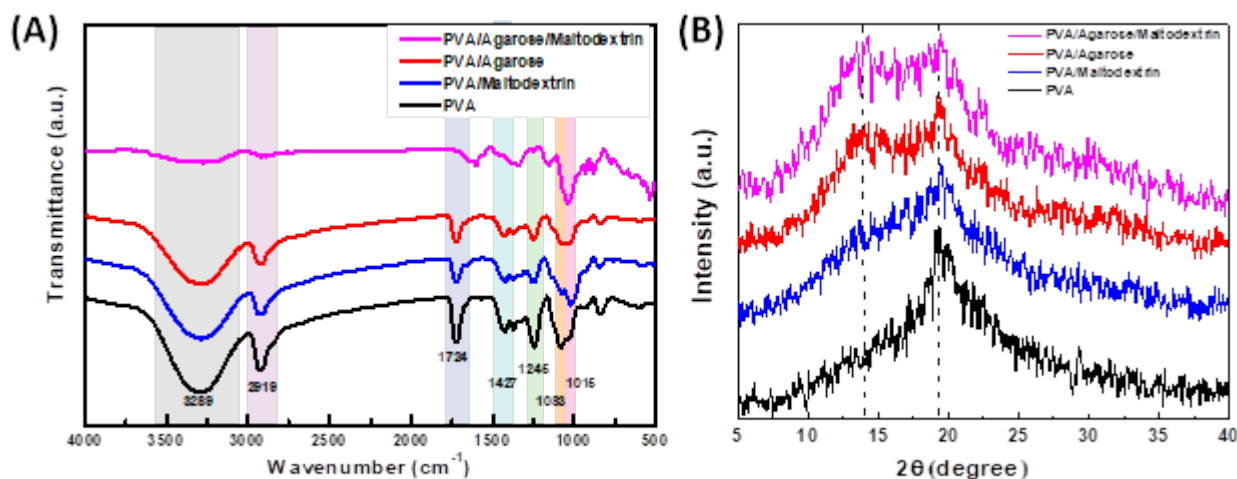


FIGURE 3. FTIR (A) and XRD pattern (B) of PVA, PVA/Agarose, PVA/Maltodextrin, PVA/Agarose/Maltodextrin membrane

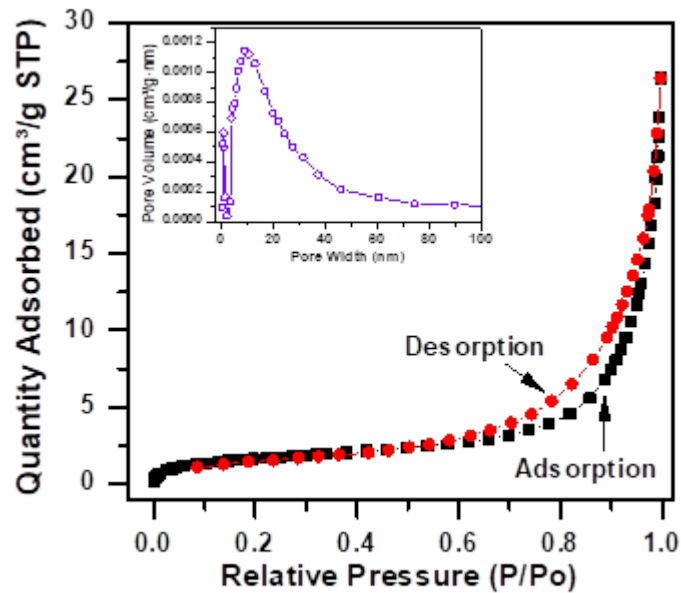


FIGURE 4. BET surface area analysis results:  $N_2$ -adsorption-desorption isotherm plots of PVA/Agarose/Maltodextrin composite membrane. Inset represents the pore size distribution results calculated from the BJH desorption pore volume data for the respective sample

#### EVALUATION OF SELECTIVE ADSORPTION

The adsorption capacity of PVA/Agarose/Maltodextrin membrane against antibiotics such as Tetracycline, Oxytetracycline, Ciprofloxacin, and Chloramphenicol was tested. As shown in Figure 5, the adsorption capacity of the materials for antibiotics is low. Ciprofloxacin showed a clear difference in adsorption capacity of antibiotics. Ciprofloxacin and Chloramphenicol adsorption capacities were recorded at 2.8 mg/g and 2.3 mg/g. For Tetracycline and Oxytetracycline antibiotics, there is almost no adsorption capacity. Therefore, the antibiotic Ciprofloxacin was used to evaluate other factors.

#### EFFECT OF TIME AND TEMPERATURE

Evaluation of influencing factors is one of the important steps to optimize the conditions and adsorption capacity of materials. The influencing factors include adsorption time, solution pH, temperature, material dosage, and antibiotic concentration. The investigated time was from 0 min to 180 min. In Figure 6(A), the adsorption process occurs rapidly over a period of 0 min to 20 min

with the adsorption capacity from 0 mg/g to 2 mg/g. The equilibrium adsorption capacity was recorded at 30 min. After 30 min, the adsorption capacity gradually decreased, indicating the desorption of the material. The temperature factor was investigated from 30 °C to 60 °C. In Figure 6(B), the adsorption capacity decreased with increasing temperature. The competition between antibiotic molecules and the material molecules has hindered the antibiotic adsorption process. The highest adsorption capacity was recorded at 1.9 mg/g at 30 °C. Therefore, the time (20 min) and the temperature (30 °C) were selected as the best adsorption condition for the next experiments.

#### EFFECT OF pH IN SOLUTION

One of the important parameters in adsorption is the solution pH, which is connected to the surface charge of the adsorbent and the antibiotic molecules. Before assessing the solution pH effect on the PVA/Agarose/Maltodextrin membrane, the pH point zero charge value was measured at 5. The pH point zero charge value < pH value of the solution indicates a negatively charged

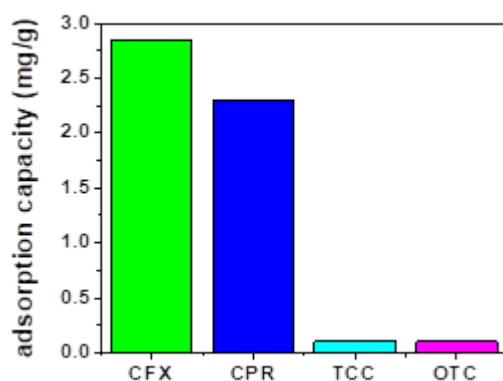


FIGURE 5. Selective antibiotic adsorption of PVA/Agarose/Maltodextrin membrane

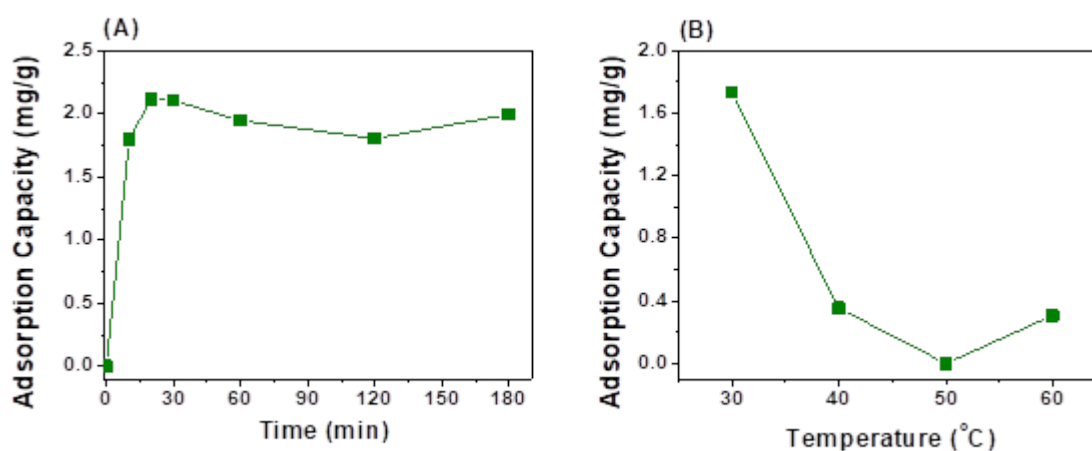


FIGURE 6. Effect of adsorption time (A) and temperature (B)

membrane surface, whereas, the pH point zero charge value  $>$  pH solution illustrates a positively charged surface (Kosmulski 2020). Based on the electrostatic repulsion theory, the pH point zero charge value can be used to explain the influence of pH on the adsorption process in the study of Thuan et al. (2019)'s group. In Figure 7(A), the medium pH influence was evaluated from pH2 to pH10, with 20 min and 30 °C. The results had a maximum value to reach at pH6 (2.7 mg/g). It can be seen that the material performs well in a neutral environment. The  $\text{pH} <$  pH of the solution showed that the material surface is negatively charged. Thus, the electrostatic interactions between positively charged Ciprofloxacin molecules and negatively charged functional groups on the PVA/Agarose/Maltodextrin membrane could promote the adsorption capacity. Therefore, the pH6 was selected

as the best medium pH value for the next evaluation experiments.

#### EFFECT OF DOSE AND CONCENTRATION

Subsequently, the dosage and concentration factors were conducted. The dose was evaluated in 4 ratios including 0.5 g/L, 1 g/L, 2 g/L, and 3 g/L. The results showed that increasing dose would lower the adsorption capacity from 4 mg/g to 7 mg/g (Figure 8). The highest dose was recorded at a concentration of 2 g/L. The concentration was evaluated from 0 mg/L to 60 mg/L. The adsorption capacity increased gradually and reached the highest point at the concentration of 40 mg/L (4.3 mg/g) (Figure 8(B)). Therefore, the dosage of 2 g/L and a concentration of 40 mg/L were used to evaluate the kinetic and isothermal models.

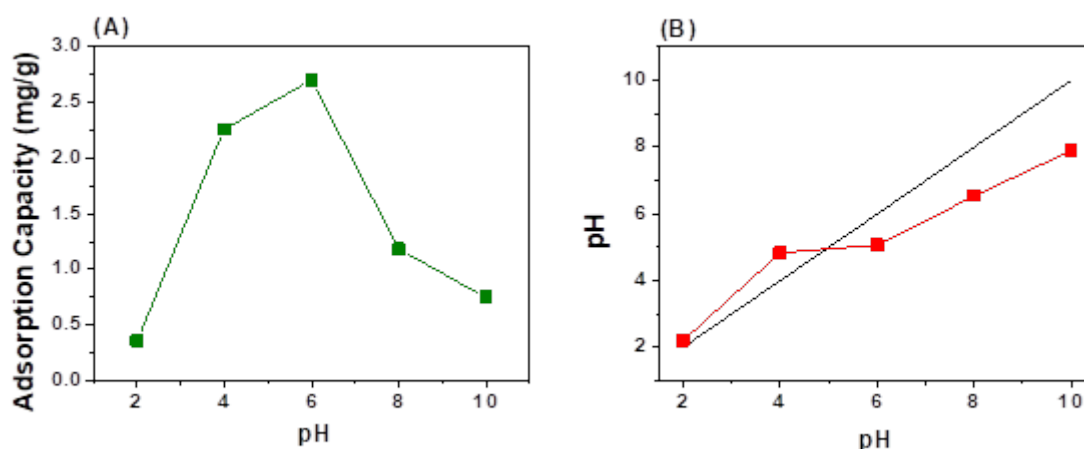


FIGURE 7. Effect of solution pH (A), pH point zero charge value (B)

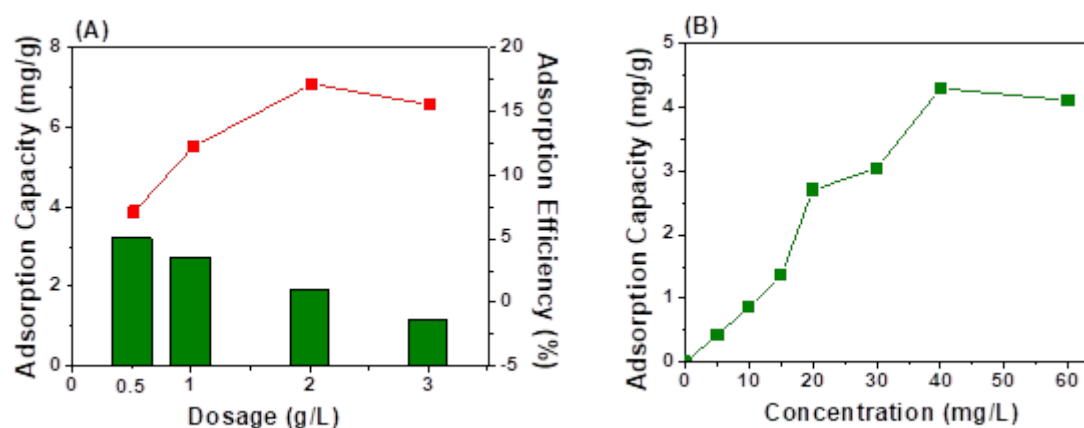


FIGURE 8. Effect of material dose (A) and antibiotic concentration (B)

#### ADSORPTION KINETICS

The parameters obtained from the adsorption kinetic model were summarized in Table 2. The kinetic model was evaluated based on the best adsorption conditions and shown in Figure 9. The PSO kinetic model was found to be the best fit with the adsorption data for the PVA/Agarose/Maltodextrin membrane, as evidenced by the highest correlation coefficient ( $R^2 = 0.975$ ) with a rate constant of 0.247 1/min. Meanwhile, the models showed almost equal coefficients. The physical adsorption process is the main reason of the formation of dense pores. These results show good agreement with the results of SEM and FTIR analysis.

#### ADSORPTION ISOTHERM

The diagrams of the isotherms were present in Figure 10 and the parameters calculated from the model were summarized in Table 3. Dubinin-Radushkevich model was best described with a high correlation coefficient ( $R^2 = 0.954$ ), while the correlation coefficients from the Freundlich model, Langmuir, and Temkin were found as 0.893, 0.923, and 0.929, respectively. The maximum adsorption capacity was recorded as 9,286 mg/g calculated from the Langmuir equation. The  $R_L$  value of 0.173 indicates that favorable adsorption was found between 0 and 1. The maximum adsorption capacity was recorded at 4,481 mg/g from the Dubinin-Radushkevich model. The adsorption process follows the Dubinin-Radushkevich model showing that the process was described by electrostatic interactions on the heterogeneous surface of the material.

TABLE 2. Kinetic parameters for the adsorption of Ciprofloxacin on PVA/Agarose/Maltodextrin membrane

	PFO	PSO	Elovich	Bangham			
$q_e$ (mg/g)	1.992	$q_e$ (mg/g)	1.988	$\theta$ (g/mg)	54.064	$k_B$ (mL/(g/L))	1.961
$k_1$ (1/min)	0.247	$k_2$ (1/min)	1.293	$\gamma$ (mg/(g.min))	4.561	$\gamma_B$	0
$R^2$	0.975	$R^2$	0.966	$R^2$	0.964	$R^2$	0.966
		$H=k_2q_e^2$	5.11				

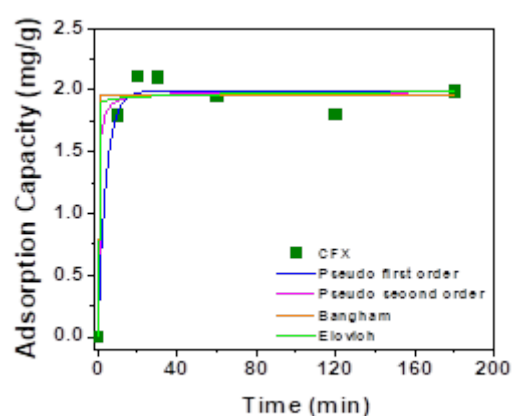


FIGURE 9. Adsorption kinetic model of PVA/Agarose/Maltodextrin membrane

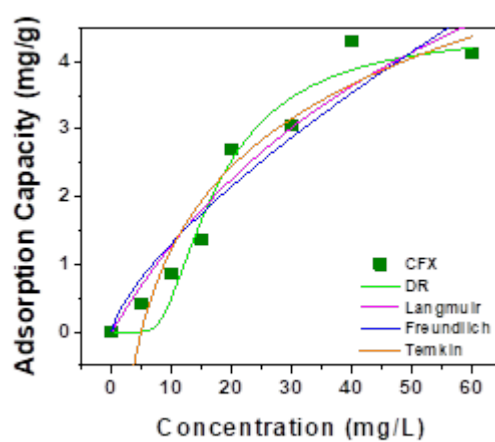


FIGURE 10. Adsorption isotherm model of PVA/Agarose/Maltodextrin membrane

TABLE 3. Isothermal parameters for the adsorption of Ciprofloxacin on PVA/Agarose/Maltodextrin membrane

Langmuir		Freundlich		Temkin		Dubinin-Radushkevich	
$K_L$ (L/mg)	0.016	$K_F$ (mg/g)	0.252	$k_T$ (L/mg)	0.202	$B$ (mol <sup>2</sup> /kJ <sup>2</sup> )	38.977
$q_m$ (mg/g)	9.286	1/n	0.715	$B_T$	1.750	$q_m$ (mg/g)	4.481
$R^2$	0.923	$R^2$	0.893	$R^2$	0.929	$R^2$	0.954
$R_L$	0.610					$E$ (kJ/mol)	62.204

## CONCLUSIONS

In this study, the PVA/Agarose/Maltodextrin membrane was synthesized and applied to adsorb antibiotics in an aqueous medium. The results obtained from SEM, XRD and FTIR analyzes show that the material has amorphous structure and pore formation. BET measurement results show that there is capillary formation inside the material. Furthermore, the results of swelling ( $431.77\% \pm 5.89$ ), solubility ( $68.88\% \pm 0.03$ ) content and contact angle ( $89^\circ$ ) have confirmed relatively high stability in aqueous media. PVA/Agarose/Maltodextrin membrane has been successfully synthesized with a higher removal efficiency of Ciprofloxacin antibiotics than other antibiotics. The Ciprofloxacin adsorption capacity of the PVA/Agarose/Maltodextrin membrane was strongly influenced by contact time, solution pH, and initial dye concentration. The highest Ciprofloxacin adsorption capacity was obtained at 20 min, 30 °C, pH6, dose 2 g/L, and initial dye concentration 40 mg/L. The Pseudo First Order and Dubinin-Radushkevich models are suitable for the adsorption kinetics and isotherms of the PVA/Agarose/Maltodextrin membrane. The maximum adsorption capacity was recorded as 4.48 mg/g based on the Dubinin-Radushkevich model.

## ACKNOWLEDGEMENTS

This research is fund by Nguyen Tat Thanh University, Ho Chi Minh city, Vietnam with code (2022.01.68/HĐ-KHCN). Author contributions is as follows: Writing-original draft preparation H.N.B.; data curation, T.C.Q.N. and H.D.T; methodology N.T.N.D; writing-review and editing L.G.B. and H.N.B. All authors have assented to the manuscript's published version.

## REFERENCES

- Abd El-Monaem, E.M., Eltaweil, A.S., M. Elshishini, H., Mohamed Hosny, Abou Alsoaud, M.M., Attia, N.F., El-Subruiti, G.M. & Omer, A.M. 2022a. Sustainable adsorptive removal of antibiotic residues by chitosan composites: An insight into current developments and future recommendations. *Arabian Journal of Chemistry* 15(5): 103743. <https://doi.org/10.1016/j.arabjc.2022.103743>
- Abd El-Monaem, E.M., Omer, A.M., Khalifa, R.E. & Eltaweil, A.S. 2022b. Floatable cellulose acetate beads embedded with flower-like Zwitterionic binary MOF/PDA for efficient removal of tetracycline. *Journal of Colloid and Interface Science* 620(August): 333-345. <https://doi.org/10.1016/j.jcis.2022.04.010>
- Abdeen, Z., Mohammad, S.G. & Mahmoud, M.S. 2015. Adsorption of Mn (II) ion on polyvinyl alcohol/chitosan dry blending from aqueous solution. *Environmental Nanotechnology, Monitoring & Management* 3: 1-9. <https://doi.org/10.1016/j.enmm.2014.10.001>
- Aslam, M., Kalyar, M.A. & Raza, Z.A. 2018. Polyvinyl alcohol: A review of research status and use of polyvinyl alcohol based nanocomposites. *Polymer Engineering & Science* 58(12): 2119-2132. <https://doi.org/10.1002/pen.24855>
- Asrofi, M., Dwilaksana, D., Abrial, H. & Fajrul, R. 2019. Tensile, thermal and moisture absorption properties of polyvinyl alcohol (PVA)/Bengkuang (*Pachyrhizuserosus*) starch blend films. *Material Science Research India* 16(1): 70-75. <https://doi.org/10.13005/msri/160110>
- Bailey, E.J. & Winey, K.I. 2020. Dynamics of polymer segments, polymer chains, and nanoparticles in polymer nanocomposite melts: A review. *Progress in Polymer Science* 105(June): 101242. <https://doi.org/10.1016/j.progpolymsci.2020.101242>
- Boczkaj, G. & Fernandes, A. 2017. Wastewater treatment by means of advanced oxidation processes at basic pH conditions : A review. *Chemical Engineering Journal*

- <https://doi.org/10.1016/j.cej.2017.03.084>
- Chang, Q., Ali, A., Su, J., Wen, Q., Bai, Y., Gao, Z. & Xiong, R. 2021. Efficient removal of nitrate, manganese, and tetracycline by a polyvinyl alcohol/sodium alginate with sponge cube immobilized bioreactor. *Bioresource Technology* 331(July): 125065. <https://doi.org/10.1016/j.biortech.2021.125065>
- Chen, C., Tang, Z., Ma, Y., Qiu, W., Yang, F., Mei, J. & Jing, X. 2018. Physicochemical, microstructural, antioxidant and antimicrobial properties of active packaging films based on poly(vinyl alcohol)/clay nanocomposite incorporated with tea polyphenols. *Progress in Organic Coatings* 123(October): 176-184. <https://doi.org/10.1016/j.porgcoat.2018.07.001>
- Dhand, V., Mittal, G., Rhee, K.Y., Park, S.-J. & Hui, D. 2015. A short review on basalt fiber reinforced polymer composites. *Composites Part B: Engineering* 73(May): 166-180. <https://doi.org/10.1016/j.compositesb.2014.12.011>
- Dieu, T.L. & Hoang, T.V. 2021. Synthesis of graphene oxide/ polyvinyl alcohol (GO/PVA) composite film as an adsorbent. *Vietnam Journal of Catalysis and Adsorption* 10(3): 6-10. <https://doi.org/10.51316/jca.2021.042>
- Ding, C. & He, J. 2010. Effect of antibiotics in the environment on microbial populations. *Applied Microbiology and Biotechnology* 87(3): 925-941. <https://doi.org/10.1007/s00253-010-2649-5>
- Falath, W., Sabir, A. & Jacob, K.I. 2017. Novel reverse osmosis membranes composed of modified PVA/gum arabic conjugates: Biofouling mitigation and chlorine resistance enhancement. *Carbohydrate Polymers* 155(January): 28-39. <https://doi.org/10.1016/j.carbpol.2016.08.058>
- Figueiredo, K.C.S., Alves, T.L.M. & Borges, C.P. 2009. Poly(vinyl alcohol) films crosslinked by glutaraldehyde under mild conditions. *Journal of Applied Polymer Science* 111(6): 3074-3080. <https://doi.org/10.1002/app.29263>
- Fu, S., Sun, Z., Huang, P., Li, Y. & Hu, N. 2019. Some basic aspects of polymer nanocomposites: A critical review. *Nano Materials Science* 1(1): 2-30. <https://doi.org/10.1016/j.nanoms.2019.02.006>
- Gao, S., Zhu, Y., Gong, Y., Wang, Z., Fang, W. & Jin, J. 2019. Ultrathin polyamide nanofiltration membrane fabricated on brush-painted single-walled carbon nanotube network support for ion sieving. *ACS Nano* 13(5): 5278-5290. <https://doi.org/10.1021/acsnano.8b09761>
- Ge, J.C., Wu, G., Yoon, S.K., Kim, M.S. & Choi, N.J. 2021. Study on the preparation and lipophilic properties of polyvinyl alcohol (PVA) nanofiber membranes via green electrospinning. *Nanomaterials* 11(10): 2514. <https://doi.org/10.3390/nano11102514>
- Ghaffari, H.R., Pasalari, H., Tajvar, A., Dindarloo, K., BakGoudarzi, B., Alipour, V. & Ghanbarnejad, A. 2017. Linear and nonlinear two-parameter adsorption isotherm modeling: A case-study. *The International Journal of Engineering and Science* <https://doi.org/10.9790/1813-0609010111>
- Ghazalian, M., Afshar, S., Rostami, A., Rashedi, S. & Bahrami, S.H. 2022. Fabrication and characterization of chitosan-polycaprolactone core-shell nanofibers containing tetracycline hydrochloride. *Colloids and Surfaces A: Physicochemical and Engineering Aspects* 636(March): 128163. <https://doi.org/10.1016/j.colsurfa.2021.128163>
- Ghemati, Dj. & Aliouche, Dj. 2014. Dye adsorption behavior of polyvinyl alcohol/glutaraldehyde/ $\beta$ -cyclodextrin polymer membranes. *Journal of Applied Spectroscopy* 81(2): 257-263. <https://doi.org/10.1007/s10812-014-9919-4>
- Hami, H., Abbas, R., Jasim, A., Abdul Abass, D., A. Abed, M. & A. Maryoosh, A. 2019. Kinetics study of removal doxycycline drug from aqueous solution using aluminum oxide surface. *Egyptian Journal of Chemistry* 62(Special Issue Part 1) Innovation in Chemistry: 91-101. <https://doi.org/10.21608/ejchem.2019.5499.1483>
- Hamoudi, S.A., Hamdi, B. & Brendlé, J. 2021. Tetracycline removal from water by adsorption on geomaterial, activated carbon and clay adsorbents. *Ecological Chemistry and Engineering S* 28(3): 303-328. <https://doi.org/10.2478/eces-2021-0021>
- Hoang, B.N., Nguyen, T.T., Nguyen, D.V. & Tan, L.V. 2021. Removal of crystal violet from aqueous solution using environment-friendly and water-resistance membrane based on Polyvinyl/Agar/Maltodextrin. *Materials Today: Proceedings* 38: 3046-3052. <https://doi.org/10.1016/j.matpr.2020.09.391>
- Hoang, B.N., Nguyen, T.T., Bui, Q.P.T., Bach, L.G., Vo, D-V.N., Trinh, C.D., Bui, X-T. & Nguyen, T.D. 2020. Enhanced selective adsorption of cation organic dyes on polyvinyl alcohol/agar/maltodextrin water-resistance biomembrane. *Journal of Applied Polymer Science* 137(30): 48904. <https://doi.org/10.1002/app.48904>
- Janani, B., Okla, M.K., Abdel-Maksoud, M.A., AbdElgawad, H., Thomas, A.M., Raju, L.L., Al-Qahtani, W.H. & Sudheer Khan, S. 2022. CuO loaded ZnS nanoflower entrapped on PVA-Chitosan matrix for boosted visible light photocatalysis for tetracycline degradation and anti-bacterial application. *Journal of Environmental Management* 306(March): 114396. <https://doi.org/10.1016/j.jenvman.2021.114396>
- Jipa, I.M., Stoica-Guzun, A. & Stroescu, M. 2012. Controlled release of sorbic acid from bacterial cellulose based mono and multilayer antimicrobial films. *LWT* 47(2): 400-406. <https://doi.org/10.1016/j.lwt.2012.01.039>
- Khandaker, S., Toyohara, Y., Kamida, S. & Kuba, T. 2018. Adsorptive removal of cesium from aqueous solution using oxidized bamboo charcoal. *Water Resources and Industry* 19(June): 35-46. <https://doi.org/10.1016/j.wri.2018.01.001>
- Kosmulski, M. 2020. The pH dependent surface charging and points of zero charge. VIII. update. *Advances in Colloid and Interface Science* 275(January): 102064. <https://doi.org/10.1016/j.cis.2020.102064>

- org/10.1016/j.cis.2019.102064
- Kumar, K., Gupta, S.C., Chander, Y. & Singh, A.K. 2005. Antibiotic use in agriculture and its impact on the terrestrial environment. *Advanced in Egronomy* 87: 1-54. [https://doi.org/10.1016/S0065-2113\(05\)87001-4](https://doi.org/10.1016/S0065-2113(05)87001-4)
- Liao, Q., Rong, H., Zhao, M., Luo, H., Chu, Z. & Wang, R. 2022. Strong adsorption properties and mechanism of action with regard to tetracycline adsorption of double-network polyvinyl alcohol-copper alginate gel beads. *Journal of Hazardous Materials* 422(January): 126863. <https://doi.org/10.1016/j.jhazmat.2021.126863>
- Lu, T., Xu, X., Liu, X. & Sun, T. 2017. Super hydrophilic PVDF based composite membrane for efficient separation of tetracycline. *Chemical Engineering Journal* 308(January): 151-159. <https://doi.org/10.1016/j.cej.2016.09.009>
- Lulijwa, R., Rupia, E.J. & Alfaro, A.C. 2020. Antibiotic use in aquaculture, policies and regulation, health and environmental risks: A review of the top 15 major producers. *Reviews in Aquaculture* 12(2): 640-663. <https://doi.org/10.1111/raq.12344>
- Madera-Santana, T.J., Freile-Pelegrín, Y. & Azamar-Barrios, J.A. 2014. Physicochemical and morphological properties of plasticized poly(vinyl alcohol)-agar biodegradable films. *International Journal of Biological Macromolecules* 69(August): 176-184. <https://doi.org/10.1016/j.ijbiomac.2014.05.044>
- Mahdavinia, G.R., Massoudi, A., Baghban, A. & Shokri, E. 2014. Study of adsorption of cationic dye on magnetic kappa-carrageenan/PVA nanocomposite hydrogels. *Journal of Environmental Chemical Engineering* 2(3): 1578-1587. <https://doi.org/10.1016/j.jece.2014.05.020>
- Maqsoudlou, A., Mahoonak, A.S., Mohebodini, H. & Koushki, V. 2020. Stability and structural properties of bee pollen protein hydrolysate microencapsulated using maltodextrin and whey protein concentrate. *Heliyon* 6(5): e03731. <https://doi.org/10.1016/j.heliyon.2020.e03731>
- Mirasgedis, S., Hontou, V., Georgopoulou, E., Sarafidis, Y., Gakis, N., Lalas, D.P., Loukatos, A., Gargoulas, N., Mentzis, A., Economidis, D., Triantafilopoulos, T., Korizi, K. & Mavrotas, G. 2008. Environmental damage costs from airborne pollution of industrial activities in the Greater Athens, Greece area and the resulting benefits from the introduction of BAT. *Environmental Impact Assessment Review* 28(1): 39-56. <https://doi.org/10.1016/j.eiar.2007.03.006>
- Mishra, S., Tiwary, D., Ohri, A. & Agnihotri, A.K. 2019. Impact of municipal solid waste landfill leachate on groundwater quality in Varanasi, India. *Groundwater for Sustainable Development* 9(October): 100230. <https://doi.org/10.1016/j.gsd.2019.100230>
- Nawar, A.M. & El-Mahalawy, A.M. 2020. Heterostructure device based on brilliant green nanoparticles-PVA/p-Si interface for analog-digital converting dual-functional sensor applications. *Journal of Materials Science: Materials in Electronics* 31(4): 3256-3273. <https://doi.org/10.1007/s10854-020-02874-1>
- Nguyen, T.T., Hoang, B.N., Tran, T.V., Nguyen, D.V., Nguyen, T.D. & Vo, D-V.N. 2021. Agar/maltodextrin/poly(vinyl alcohol) walled montmorillonite composites for removal of methylene blue from aqueous solutions. *Surfaces and Interfaces* 26(October): 101410. <https://doi.org/10.1016/j.surfin.2021.101410>
- Ololade, O.O., Mavimbela, S., Oke, S.A. & Makhadi, R. 2019. Impact of leachate from northern landfill site in bloemfontein on water and soil quality: Implications for water and food security. *Sustainability* 11(15): 4238. <https://doi.org/10.3390/su11154238>
- Przydatek, G. & Kanownik, W. 2019. Impact of small municipal solid waste landfill on groundwater quality. *Environmental Monitoring and Assessment* 191(3): 169. <https://doi.org/10.1007/s10661-019-7279-5>
- Ramakrishna, S., Mayer, J., Wintermantel, E. & Leong, K.W. 2001. Biomedical applications of polymer-composite materials: A review. *Composites Science and Technology* 61(9): 1189-1224. [https://doi.org/10.1016/S0266-3538\(00\)00241-4](https://doi.org/10.1016/S0266-3538(00)00241-4)
- Rodríguez-San-Miguel, D. & Zamora, F. 2019. Processing of covalent organic frameworks: An ingredient for a material to succeed. *Chemical Society Reviews* 48(16): 4375-4386. <https://doi.org/10.1039/C9CS00258H>
- Rynkowska, E., Fatyeyeva, K., Marais, S., Kujawa, J. & Kujawski, W. 2019. Chemically and thermally crosslinked PVA-based membranes: Effect on swelling and transport behavior. *Polymers* 11(11): 1799. <https://doi.org/10.3390/polym11111799>
- Sabarish, R. & Unnikrishnan, G. 2018. Polyvinyl alcohol/carboxymethyl cellulose/ZSM-5 zeolite biocomposite membranes for dye adsorption applications. *Carbohydrate Polymers* 199(November): 129-140. <https://doi.org/10.1016/j.carbpol.2018.06.123>
- Saha, N., Volpe, M., Fiori, L., Volpe, R., Messineo, A. & Toufiq Reza, M. 2020. Cationic dye adsorption on hydrochars of winery and citrus juice industries residues: Performance, mechanism, and thermodynamics. *Energies* 13(18): 4686. <https://doi.org/10.3390/en13184686>
- Shamsuri, A.A. & Daik, R. 2013. Utilization of an ionic liquid/urea mixture as a physical coupling agent for agarose/talc composite films. *Materials* 6(2): 682-698. <https://doi.org/10.3390/ma6020682>
- Sritham, E. & Gunasekaran, S. 2017. FTIR spectroscopic evaluation of sucrose-maltodextrin-sodium citrate bioglass. *Food Hydrocolloids* 70(September): 371-382. <https://doi.org/10.1016/j.foodhyd.2017.04.023>
- Thuan, V.T., Bich, N.H., Hien, T.T., Nhan, P.T.N., Van, T.T.H., Hai, N.D., Cao, V.D., Nguyen, T.D. & Bach, L.G. 2019. Activated carbon via pyrolysis of tea industry waste biochar with KOH activation: Preparation and characterization. *Journal of Engineering and Applied Sciences* 14(6): 1755-

1759. <https://doi.org/10.36478/jeasci.2019.1755.1759>
- Tian, H., Yan, J., Rajulu, A.V., Xiang, A. & Luo, X. 2017. Fabrication and properties of polyvinyl alcohol/starch blend films: Effect of composition and humidity. *International Journal of Biological Macromolecules* 96: 518-523. <https://doi.org/10.1016/j.ijbiomac.2016.12.067>
- Tran, H.N., You, S.-J., Hosseini-Bandegharaci, A. & Chao, H.-P. 2017. Mistakes and inconsistencies regarding adsorption of contaminants from aqueous solutions: A critical review. *Water Research* 120(September): 88-116. <https://doi.org/10.1016/j.watres.2017.04.014>
- Uppuluri, V.N.V.A. & Shanmugarajan, T.S. 2019. Icarin-loaded polyvinyl alcohol/agar hydrogel: Development, characterization, and in vivo evaluation in a full-thickness burn model. *The International Journal of Lower Extremity Wounds* 18(3): 323-335. <https://doi.org/10.1177/1534734619849982>
- Wang, W., Dai, Y., Zhang, H., Zhang, R., Hou, H. & Dong, H. 2018. Effects of hydrophobic agents on the physicochemical properties of edible agar/maltodextrin films. *Food Hydrocolloids* <https://doi.org/10.1016/j.foodhyd.2018.10.008>
- Wu, M., Zhao, S., Jing, R., Shao, Y., Liu, X., Lv, F., Hu, X., Zhang, Q., Meng, Z. & Liu, A. 2019. Competitive adsorption of antibiotic tetracycline and ciprofloxacin on montmorillonite. *Applied Clay Science* 180(November): 105175. <https://doi.org/10.1016/j.clay.2019.105175>
- Yan, C., Fan, L., Chen, Y. & Xiong, Y. 2020. Effective adsorption of oxytetracycline from aqueous solution by lanthanum modified magnetic humic acid. *Colloids and Surfaces A: Physicochemical and Engineering Aspects* 602(October): 125135. <https://doi.org/10.1016/j.colsurfa.2020.125135>
- Yang, W., Fortunati, E., Bertoglio, F., Owczarek, J.S., Bruni, G., Kozanecki, M., Kenny, J.M., Torre, L., Visai, L. & Puglia, D. 2018. Polyvinyl alcohol/chitosan hydrogels with enhanced antioxidant and antibacterial properties induced by lignin nanoparticles. *Carbohydrate Polymers*. <https://doi.org/10.1016/j.carbpol.2017.10.084>
- Yang, X., Zhu, Z., Liu, Q., Chen, X. & Ma, M. 2008. Effects of PVA, agar contents, and irradiation doses on properties of PVA/Ws-chitosan/glycerol hydrogels made by  $\gamma$ -irradiation followed by freeze-thawing. *Radiation Physics and Chemistry* 77(8): 954-960. <https://doi.org/10.1016/j.radphyschem.2008.02.011>
- Yazidi, A., Atrous, M., Soetaredjo, F.E., Sellaoui, L., Ismadji, S., Erto, A., Bonilla-Petriciolet, A., Dotto, G.L. & Ben Lamine, A. 2020. Adsorption of amoxicillin and tetracycline on activated carbon prepared from durian shell in single and binary systems: Experimental study and modeling analysis. *Chemical Engineering Journal* 379(January): 122320. <https://doi.org/10.1016/j.cej.2019.122320>
- Zhao, Y., Li, X., Shen, J., Gao, C. & Van der Bruggen, B. 2020. The potential of kevlar aramid nanofiber composite membranes. *Journal of Materials Chemistry A* 8(16): 7548-7568. <https://doi.org/10.1039/D0TA01654C>

\*Corresponding author; email: blgiang@ntt.edu.vn